DECORATED GRAPHENE OXIDE WITH OCTADECYL AMINE/SASOBIT/EPOXY NANOCOMPOSITE VIA VACUUM SHOCK TECHNIQUE: MORPHOLOGY AND BEAMS SHIELDING

Seyyed Mojtaba Mousavi[1,2], Seyyed Alireza Hashemi[1,2], Younes Ghasemi[1,2]

[1] *Department of Medical Nanotechnology*
 School of Advanced Medical Sciences and Technologies
 Shiraz University of Medical Sciences, Shiraz, Iran
[2] *Pharmaceutical Sciences Research Center*
 Shiraz University of Medical Sciences, Shiraz, Iran
 71348-14336
 E-mail: s.a.hashemi0@gmail.com
 sa_hashemi@sums.ac.ir

ABSTRACT

Herein, graphene oxide (GO) nanoparticles were fabricated via Improved Hummers method. Then, the fabricated GO nanoparticles were modified by octadecyl amine (ODA) through multi-step procedure in order to improve their optoelectrical activity. In this case, modification of GO with ODA (GO-ODA) was conformed via FTIR analysis. Afterward, through the modified vacuum shock technique, nanocomposites containing Sasobit along with GO and GO-ODA were fabricated at different filler loadings. UV-Vis light spectroscopy results showed that the modification of GO with ODA can enhance the visible light absorption rate, while it can perfectly absorb UV beams. Despite, addition of Sasobit along with GO and GO-ODA can lead to significant increase in the whole UV-vis light region and overlap the low visible light absorption rate of both GO and GO-ODA. Eventually, with cost affordable materials such as Sasobit along with GO and GO-ODA, high absorption rate in the UV-Vis light region can be obtained. In fact, by development of these kinds of shields, practical barriers against harmful beams such as UV can be achieved.

Keywords: graphene oxide, octadecyl amine, Sasobit, nanocomposite, optical properties.

INTRODUCTION

Since the discovery of graphene in 2004 [1] and due to its unique properties in variety of fields such as exceptional electric conductivity [1 - 3], perfect optical properties [4], appropriate light transmission and high surface area [5, 6], it has become a reliable candidate for reinforcing polymeric based nanocomposites. The graphene is known as a one thick, 2D crystal lattice containing sp^2 hybridized carbon atoms in a heterocyclic structure [7, 8]. Moreover, a single graphene layer known as semi-metal or zero gap semiconductor that can provide unique electronic behavior with electron mobility ranging from 3000 to 27000 $cm^2/V.s$ at room temperature (RT) which can transmit of about 97.7 % of incident light beams [9, 10].

In addition, graphene oxide (GO) consisted from few graphene layers decorated with active functional groups such as hydroxyl, carboxyl, epoxy and oxygen-based functional groups [11] which can improve their dispersion quality within the polymeric matrix [12]. These active functional groups can deteriorate the electrical conductivity of GO due to the break of sp^2 networks within the GO structure. Furthermore, the sign of transition from insulation to conductivity for GO is accompanied with change in the optical properties which its band structure and thus optical properties is highly depend on the overall amount of oxygen groups coverage [13, 14].

Besides, GO is an effective electron mediator due to its extending interface to the whole area of graphene sheets which can boost the charge migration and thus

extend the lifetime of photo-generated charges [15 - 17]. Moreover, π-π stacking interaction between GO and molecularly attached particles on its surface and improvement of photo generated charges due to the acceleration of interfacial electron transfer rate can improve the optical activity of modified GO [18]. Additionally, larger surface area for GO can improve active sites on its surface, while defects such as oxygen vacancies in the GO structure not only can produce trapped sites but also can repress electron-hole pair recombination by capturing electrons [19]. On the other hand, functionalization of GO nanoparticles with octadecyl amine (ODA) can decrease the overall amount of oxygen based functional groups which can improve the structural quality and electrical conductivity of GO nanoparticles [20 - 22]. In a work by Li et al. [20], they were functionalized GO with ODA by a simple refluxing procedure without usage of any reducing agent. In this regard, the modification of GO with ODA led to reduction of GO and thus improvement of electrical conductivity as well as increase in the dispersion quality within the polymeric matrix. In another work by Pang et al. [22], they fabricated GO-ODA/ carbon nanotube (CNT)/polyethylene composite with a segregated and double-percolated structure. The results of their study revealed that the addition of a low amount of GO-ODA (0.06 vol. %) along with CNT can lead to a significant improvement in the electrical conductivity, yield strength and tensile modulus of developed specimens. In a work by Schöche et al. [11], they reported the optical constants of graphene oxide and reduced graphene oxide (rGO) determined by spectroscopic ellipsometry. In this case, the anisotropic optical constants of GO were precisely determined from a multi-sample analysis of data obtained from a thick drop-cast layer. The optical properties of rGO vary with respect to divers reduction procedures which depend on residual oxygen groups coverage and defects within the graphitic flakes. Moreover, increase in the intensity of functional groups can lead to a decrease in the optoelectrical properties of graphene which can be furtherly enhanced via reduction process. In fact, reduction process will enhance the optoelectrical properties by decreasing the overall amount of oxygen-based functional groups.

In another work by Cruz-Ortiz et al. [23], the effectiveness of titania-graphene composites under UV-Vis light irradiation was investigated. In this matter, TiO_2 – reduced graphene oxide composites (TiO_2 - rGO) were prepared through the photocatalytic reduction of exfoliated GO using P25 (Evonik-Aeroxide) as the photocatalyst. TiO_2 - rGO composites can improve the solar photocatalytic efficiency due to different possible mechanisms including: charge separation improving and reduction of electron hole recombination rates; changing the ROS distribution and inducing visible light activity due to the presence of Ti-O-C bonds giving mid gap states above the valence band gap [23 - 25]. In a study by Goumri et al. [12], the electrical and optical properties of rGO and multiwalled carbon nanotube (MWCNT) nanocomposites were investigated. In this work, in situ rGO/Poly (vinyl alcohol)/MWCNT/Sodium Dodecyl Sulfate/Poly (vinyl alcohol) composites were prepared via water dispersion and divers reduction treatments. In this regard, high absorption rate was observed in near UV regions and the photoluminescence enhancement was achieved at 1 wt. % graphene loading, while the carbon nanotubes (CNT) based composite presents a significant emission at 0.7 wt. % followed with a photoluminescence quenching at higher fraction of the nanofillers (1.6 wt. % TRGO and 1 wt. % MWCNT). Khan et al. [26] investigated the optical and electrical properties of decorated rGO sheets with Ag nanoparticles. Their results showed that attachment of Ag nanoparticles on the surface of rGO can lead to a significant improvement (ten times higher) in the electrical conductivity as well as optical properties, while the optical transmittance improved about 90 % compared with 70 % improvement before attachment of Ag nanoparticles to the rGO.

Additionally, Sasobit is an organic synthetic microcrystalline wax with long chain length of aliphatic hydrocarbons with 40 - 114 carbon atoms and fine crystalline structure [27, 28]. Sasobit has registered in chemical abstract service (CAS) with code 8002-74-2 and its chemical formula is C_nH_{2n+2}. Moreover, Sasobit is obtaining from Sasol wax which can be find in the South Africa and the common procedure technique for its fabrication is via Fischer-Tropsch method [27]. The chemical reaction which can lead to the production of Sasobit is as follows [29]:

$$(2n + 1)H_2 + nCO_2 \rightarrow C_nH_{2n+2} + nH_2O \quad (1)$$
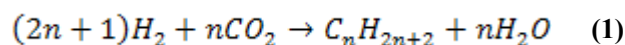
Besides, long chain length of the aliphatic hydrocarbons in Sasobit can lead to decrease in the viscosity and construction temperature of the final suspension.

Wider chain length range not only can extend the plastic limit but also improve the melting temperature of various kinds of matrices. Moreover, Sasobit can provide perfect thermal resistance for composites along with its affordable cost [27]. Recently, diverse kinds of matrices were used to develop practical composites for variety of applications, among we can refer to the phenol novolac epoxy resin modified with unsaturated polyester (PNE/UPS) [30], linear low-density-polyethylene (LLDPE) [31], epoxy resin [32 - 38], cresol novolac epoxy resin modified with unsaturated polyester (CNP/UPS) [39] and polyethylene terephthalate (PET) [40]. These matrices suffer from some disadvantages which needs higher level of attention.

Herein, we have developed GO nanoparticles via improved Hummers method and then decorated GO with octadecyl amine by replacement of amine groups with oxygen-based functional groups. Thereafter, specimens containing diverse filler loadings of GO, GO-ODA and Sasobit were developed using vacuum shock technique. Then, effectiveness of developed specimens in matter of UV-Vis light absorption was examined and reported.

EXPERIMENTAL
Materials and methods

GO was prepared via improved Hummers method [41]. In this case, all of required ingredients such as H_2SO_4, H_3PO_4, HCl, H_2O_2, $KMNO_4$ and Graphite were supplied by Merck & Co. Moreover, via a multi stage manufacturing procedure, GO nanoparticles were deco-

rated with ODA functional group. For this purpose, ODA nanoparticles, ethanol and NH_3 were supplied by Merck & Co. In the next part, via vacuum shock technique [35, 42], nanocomposite containing GO, GO-ODA and Sasobit at different filler loadings were fabricated. Nanocomposites specification and filler loadings are given in Table 1. For the production of nanocomposites, NPEL-128 or NAN YA-128 epoxy resin (supplied by Nan Ya Plastic Corp.) was used as matrix and cured with curing agent EPIKURE™ F205 (supplied by Hexion) according to considered procedure. Besides, acetone (supplied by Merck) and E-10 Cardura (supplied by Hexion) was used as dispersant and diluent agents, respectively.

For evaluation of the fabricated nanoparticles, FTIR (Bruker model VECTOR22) analysis was conducted. Furthermore, nanocomposites morphology and structural condition were examined using SEM (TESCAN model VEGA3 SB) analysis. In order to evaluate the performance of developed nanocomposites towards UV-Vis light absorption, UV-Vis spectrophotometer (model Shimadzu-1800) was used.

Materials preparation
Fabrication of GO nanoparticles

In order to synthesis GO nanoparticles, first 2 L H_2SO_4 was poured in a round-bottom flask and stirred (500 rpm) at temperature of about 0 - 5°C. Then, 50 g $KMNO_4$ was added to the H_2SO_4 and afterward 10 g graphite was slowly added to the previous suspension. In the following step, 110 cc H_3PO_4 was added to the

Table 1. Specification of the developed nanocomposites.

Sample Number	Filler loading (wt. %)		
	GO	GO-ODA	Sasobit
1	0	0	1
2	0	0	3
3	0	0	5
4	0.5	0	0
5	0.5	0	1
6	0.5	0	3
7	0.5	0	5
8	0	0.5	0
9	0	0.5	1
10	0	0.5	3
11	0	0.5	5
12	Pure Epoxy Resin		

previous suspension and then the suspension was stirred (500 rpm) for 72 h at 50°C, respectively. Thereafter, the resulting suspension was poured in a vacuum Erlenmeyer flask and some ice cubes (made from deionized water) were poured into the flask. Thereupon, 10 cc H_2O_2 was poured into the suspension very slowly and then the vacuum Erlenmeyer flask was filled with deionized water. Resulting suspension was kept without stirring for 48 h, for further fillers sediment. Afterward, the suspension was washed with HCl in order to remove metal ions and then filtered and remained fillers on the filter paper washed with deionized water in order to set pH on 7. Resulting nanoparticles were dried for 1 h under 100°C in the heat oven and then placed in a humidity absorbing chamber for 48 h for further humidity reduction.

Modification of GO with ODA

In the next stage, GO nanoparticles were decorated with ODA via the following procedure. In this regard, first 0.9 g ODA nanoparticles ultrasonicated in 90 ml ethanol at 300 W for 10 min with simultaneous cool in an ice bath (45°C temperature limit). Then 0.6 g GO nanoparticles were added to the previous suspension and ultrasonicated at 300 W for 10 min (50°C temperature limit). Afterward, 300 ml deionized water was added to the resulting suspension ultrasonicated at 400 W for 30 min (60°C temperature limit). In the next step, resulting suspension was poured into a round-bottom flask and stirred (500 rpm) for 1 h at 80°C. Then, 3 ml NH_3 was added to the suspension and stirred (500 rpm) at 80°C for 48 h. Final suspension was vacuum filtered and pH of the developed nanoparticles were set on 7 via simultaneous washing with deionized water. Thereafter, developed GO-ODA nanoparticles were placed in a heat oven for 1 h at 100°C and then placed in a humidity absorbing chamber for 48 h, respectively.

Nanocomposites preparation

Nanocomposites containing GO, GO-ODA and Sasobit at different filler loadings were fabricated via vacuum shock technique [35]. Specification of these nanocomposites can be seen in Table 1. In this case, related fillers were ultrasonicated in 100 ml acetone for 30 min at 300 W. Then, the resulting suspension containing fillers/acetone and epoxy resin were poured in a vacuum Erlenmeyer flask and stirred (500 rpm) for 3 h under 10 - 60 cm Hg vacuum shock. Afterward, indirect heat

of about 80°C added to the previous step's suspension and the dispersion lasted for further 1:30 h. In the next step, curing agent and E-10 Cardura were scaled with ratio 100:40 (wt. % : wt. %) and 100:10 (wt. % : wt. %) with respect to the matrix, respectively. Then, the resulting suspension and curing agent along with E-10 were separately placed in the vacuum chamber under vacuum shock varies between 25 - 50 cm Hg for 30 min for further bubble reduction. In the following step, resulting suspension and curing agent were mixed and stirred (200 rpm) for 5 min and then placed under vacuum shock between 25 - 50 cm Hg for 10 min. Afterward, E-10 Cardura was added to the suspension and stirred (200 rpm) for 5 min and then placed under another vacuum shock between 25 - 50 cm Hg for 5 min. Addition of E-10 to the suspension can apply a shock to matrix viscosity. In this case, it can lead to a rapid decrease in the matrix viscosity which can provide the possibility for internal pressure of bubbles to overcome their boundary areas in the radial directions. Eventually, it can lead to diffusion of air from bubbles to the matrix, reduce in bubbles size and thus collapse of bubbles which creating due to the reaction between matrix and curing agent, respectively. In the next stage, suspension was poured in related molds and cured in 3 steps. First at room temperature for 7 h, then at heating range of about 30 - 40°C for 24 h and finally for 1 h under 100°C. Moreover, along with acetone and E-10 in production procedure, addition of Sasobit to the suspension can decrease the viscosity of matrix [27] and thereby can improve the dispersion quality of fillers within the matrix.

RESULT AND DISCUSSION
FTIR examination of produced nanoparticles

FTIR examination of GO, ODA and GO-ODA can be seen in Fig. 1. Typical peaks for GO are ∼580 cm⁻¹ (C=O), ∼846 cm⁻¹ (C-H sp²), ∼887 cm⁻¹ (germinal distribution), ∼1004 cm⁻¹ (vibration of a p-disubstituted phenyl group (v_{C-H} in plane bending)), ∼∼1059 cm⁻¹ (C-O in epoxide), ∼1173 cm⁻¹ (C-OH in alcohol or C-C-N amines or C-OC in ether), ∼1626 cm⁻¹ (C=C bonds (sp² C-X double bonds) in aromatic ring), ∼1727 cm⁻¹ (C=O carboxylic stretching vibration) and 3410 cm⁻¹ (-OH in alcohols and phenols, OH stretch (solid), intermolecular bonded). Besides, for ODA, peaks between range ∼2849 - ∼3000 cm⁻¹ and at ∼1462 cm⁻¹ are corresponding to the C-H. Moreover, other appeared

peaks ∿∿719, ∿∿1063 and ∼1627 cm⁻¹ are resulting from exist of C-H, C-O stretching (primary alcohol) and C=C, respectively. Successful functionalization of GO with ODA could be due to several reasons such as hydrogen bonding, electrostatic attraction between carboxylic group and protonated amine and also nucleophilic substitution between epoxy group and protonated amine which amine groups acting as a nucleophile and hitting carbon atoms [21]. Besides, the exist of hydroxide and carboxylic groups on the surface of fabricated GO nanoparticles can provide the possibility for hydrogen bonding and electrostatic attraction between GO and ODA. Largest intensity change in the GO-ODA spectrum is related to peaks ∼2849 - ∼3000 cm⁻¹ and 1462 cm⁻¹, corresponding to the C-H stretching and deformation, respectively, which is due to the introduction of long hydrocarbons chain to the GO's surface [21]. Appearance of peaks ∼2849 - ∼3000 cm⁻¹ from the -CH₂ stretching of the octadecyl chain along with 720 cm⁻¹ peaks show successful modification of GO nanoparticles with ODA [20 - 22]. Additionally, the presence of new peaks at 1467 cm⁻¹ (C-N stretch of amide) and 1591 cm⁻¹ (N-H bending of amide) in the GO-ODA spectrum indicated that amide carbonyl bonds were created between the GO flakes and ODA molecules [20, 43]. Furthermore, peaks between region 1030 - 1160 cm⁻¹ (C-O-C) and 1591 cm⁻¹ (N-H stretching vibration) which were weakened and appeared in the GO-ODA spectrum, respectively, indicating the formation of -C-NH-C bonds due to the reaction between epoxide groups and amine groups [20]. In addition, the disappearance of peak at 1720 cm⁻¹ which is corresponding to the carboxylic group, indicated the interaction of carboxylic groups with ODA molecules. Moreover, reaction of epoxide groups with ODA molecules can lead to the generation of C-OH and C-N bonds [21].

SEM examination of developed nanocomposites

In order to examine the structural quality and morphology of fabricated nanocomposites, SEM analysis was conducted. SEM images of nanocomposites at different filler loadings are shown in Fig. 2. As can be seen in Fig. 2(a-c), by increase in the Sasobit weight percentage within the matrix, the roughness of the fabricated nanocomposites was increased. This result was also the same for nanocomposites containing GO and Sasobit at different filler loadings (Fig. 2 (e-g)). Moreover, addition of GO-ODA nanoparticles to nanocomposites along with Sasobit particles, can improve the morphology and make the surface of fabricated nanocomposites a bite smoother (Fig. 2(i-k)). As can be seen in Fig. 2(i-k), nanocomposites containing GO-ODA showing smoother surface and thus lower roughness rate compared with other specimens. In addition, sample containing GO-ODA (Fig. 2(h)) shows smoother surface than samples containing GO (Fig. 2(d)) and neat epoxy resin (Fig. 2(l)). Eventually, the modification of GO with ODA nanoparticles not only can improve the dispersion quality of GO nanoparticles due to the presence of various kind of functional groups but also enhance the structural quality and decrease the surface roughness of developed nanocomposites.
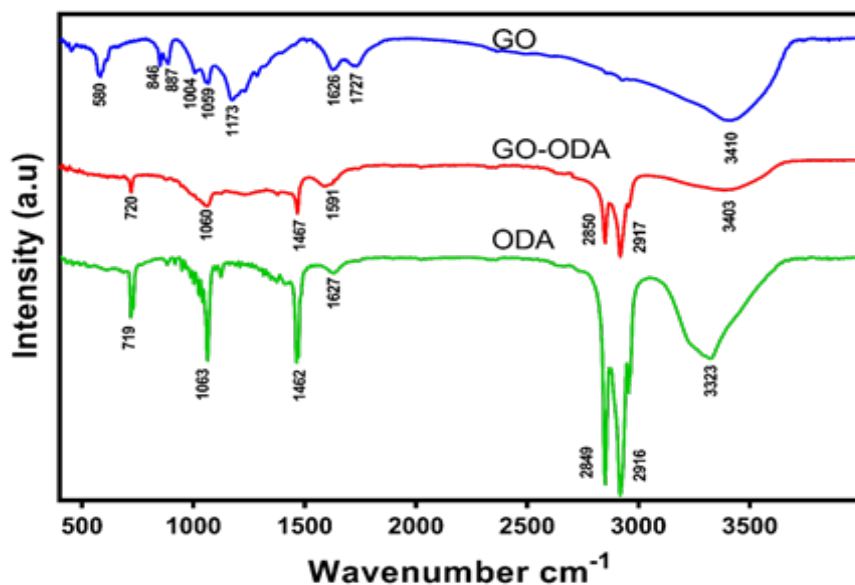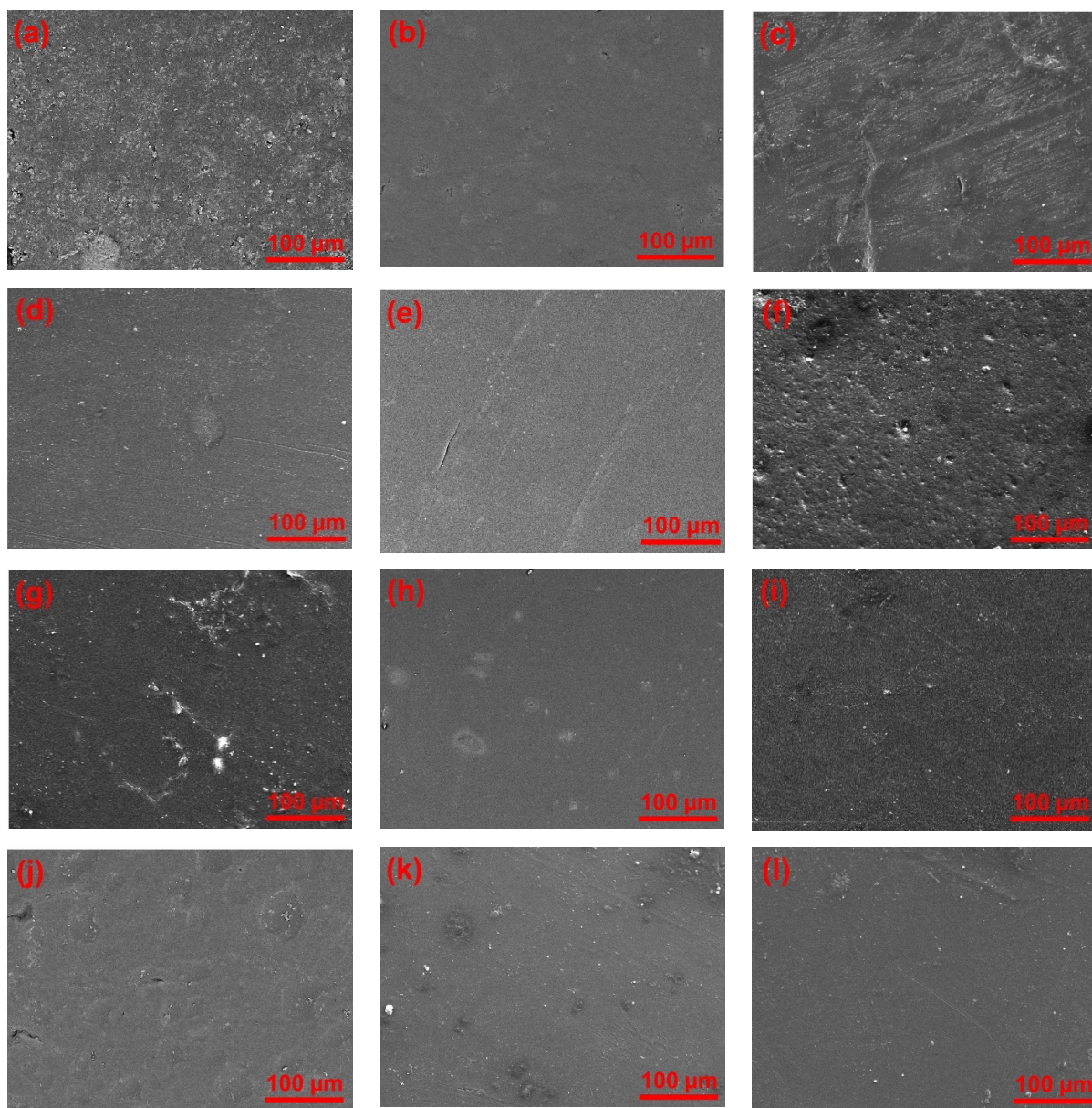

Fig. 1. FTIR results for GO, GO-ODA and ODA.

Fig. 2. SEM images of nanocomposites containing diverse filler loadings of GO, GO-ODA and Sasobit; sample 1 (a), sample 2 (b), sample 3 (c), sample 4 (d), sample 5 (e), sample 6 (f), sample 7 (g), sample 8 (h), sample 9 (i), sample 10 (j), sample 11 (k), sample 12 (l).

UV-Vis light absorption

When a light or photon is hitting a conductive surface, a valence or core electron is excited to the conductive or higher unoccupied energy band and the electron becomes a photo excited electron. This phenomenon is the main reason for optical, UV and X-ray absorption which mainly depend on the energy of the photon. Besides, the electrical interaction of the photon-absorption process is generally called electrical dipole interaction [44]. Occupied state of the photon-excited electron becomes unoccupied due to the optical absorption in valence or core energy band and this unoccupied region becomes like a particle with positive charge, which called hole. Moreover, coulomb interaction force between photon-excited electron and hole can lead to creation of a bound state which called valence or core exciton [45]. Furthermore, the photon-excited electron or hole can be scattered by emitting photons due to the excited-photon or electron photon interactions. This phenomenon can lead to the relaxation of excitations to the bottom of

conduction or top of valence band. Moreover, after a time of about 10 ps -1 ns, the photon-excited electron and the hole recombine by emission of a photon due to the spontaneous emission of a photon which is known as photoluminescence (PL). These processes which including photon absorption, relaxation and photon emission is called optical process. Additionally, a photon can be either emitted by PL or light scattering process. Change in the momentum of the incident light or overall amount of energy in the presence of a material can lead to the light scattering by the target material. Scattered light is very necessary to recognize the color of the material. The scattering phenomenon is consisted from serial of optical processes such as optical absorption, scatter of a photon-excited electron and photon emission. Likewise, light scattering phenomenon is 1000 times faster (10 fs -1 ps) than PL (10 ps -1 ns). There are two different kinds of scattering processes such as elastic and inelastic

scattering of light, which are known as Rayleigh and Raman Scattering, respectively [44].

Rayleigh scattering occurs due to the vibration of dipole moment which is induced in a material by the incident light. This phenomenon can lead to the generation of an electromagnetic wave due to the vibrating dipole moment and scattered photon propagates into various directions from the direction of incident photon without losing any energy. This phenomenon is very fast (10 fs) and has spectral width of about 100 cm^{-1} (11.6 meV). Besides, Raman scattering occur due to the inelastic scattering of the light. In this regard, the photon excited electron loses or gain energy due to the absorption of some elementary excitation such as phonons or via exciting another exciton or by exciton-phonon or exciton-exciton interaction. In this situation, the scattered light loses or gain energy from the exciton which is known as stoke and anti-stoke shifts of light [44, 46].
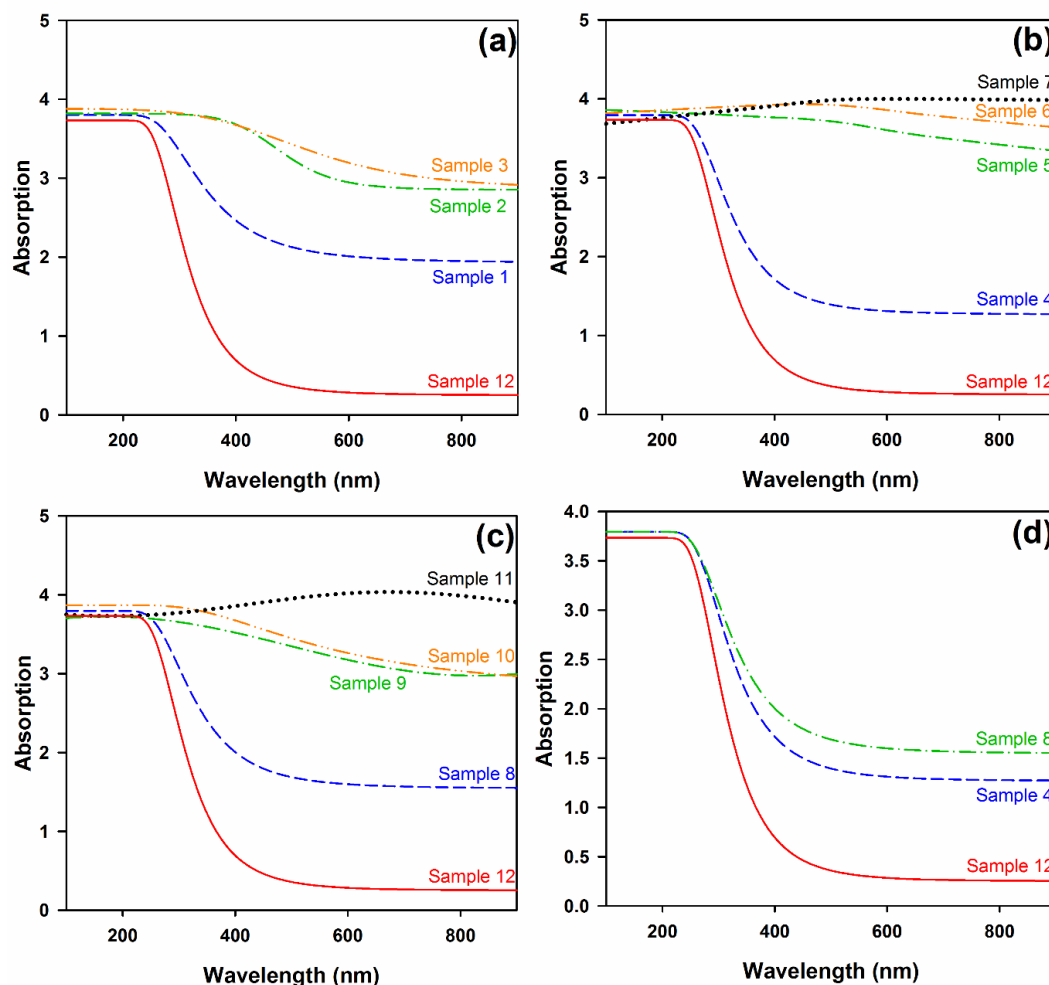

Fig. 3. UV-Vis light absorption rate of nanocomposites at different filler loadings.

In addition, UV-Vis light absorption rate of developed specimens at different filler loadings is shown in Fig. 3. In Fig. 3(a), UV-Vis light absorption rate for nanocomposites containing Sasobit at different filler loadings (1, 3 and 5 wt. %) can be seen. As can be seen, the increase in the weight percentage of Sasobit can lead to significant increase in the overall amount of UV-Vis light absorption rate. In Figs. 3(b) and (c), the effect of Sasobit along with GO and GO-ODA on UV-Vis light spectrum can be seen, respectively. As shown in these figures, addition of Sasobit to nanocomposites along with GO and GO-ODA led to significant improvement in visible light spectrum as well as UV spectrum. In Fig. 3(d), UV-Vis light absorption rates of GO and GO-ODA are compared with net epoxy matrix. As shown, the decoration of GO with ODA led to significant improvement in the visible light region. In fact, π-π stacking interaction between GO and ODA and decrease in the overall intensity of functional groups such as carboxyl, hydroxyl, epoxide and other oxygen based functional groups due to the interaction with long hydrocarbon chains of ODA led to improvement in the optoelectronic activity of GO. Despite, as well as increase in the optoelectronic activity, modification of GO with ODA can improve its dispersion quality through the matrix [20]. Eventually, addition of Sasobit along with GO-ODA can significantly improve the capacity of nanocomposites in matter of UV-vis light absorption. These cost affordable and effective additives can be furtherly used for development of shields in matter of UV protection.

CONCLUSIONS

In this study, GO nanoparticles were fabricated via improved Hummers method and then functional groups of GO were replaced with ODA to improve its optoelectrical activity. Afterward, nanocomposites containing GO, GO-ODA and Sasobit at different fillers loading were fabricated using modified vacuum shock technique. Outcome of evaluations showed that modification of GO with ODA not only can decrease the overall amount of functional groups and replace them with ODA but also can improve the optoelectronic activity of GO in visible light region and increase the dispersion quality of modified GO within the matrix. Moreover, addition of Sasobit along with GO and GO-ODA can lead to significant increase in the UV-Vis light absorption rate. Eventually,

with cost affordable materials such as Sasobit along with GO and GO-ODA, nanocomposites with significant high absorption rate in the whole UV-Vis light region can be obtained, which can be furtherly used as barrier against harmful beams such as UV.

REFERENCES

1. K.S. Novoselov, A.K. Geim, S.V. Morozov, D. Jiang, Y. Zhang, S.V. Dubonos, I.V. Grigorieva, A.A. Firsov, Electric field effect in atomically thin carbon films, Science, 306, 5696, 2004, 666-669.
2. A.K. Geim, K.S. Novoselov, The rise of graphene, Nature materials, 6, 3, 2007, 183-191.
3. J. Marzouk, B. Lucas, T. Trigaud, A. Pothier, J. Boucle, B. Ratier, Simple strategy to tune the charge transport properties of conjugated polymer/carbon nanotube composites using an electric field assisted deposition technique, Polymer International, 63, 8, 2014, 1378-1386.
4. J. Shang, L. Ma, J. Li, W. Ai, T. Yu, G.G. Gurzadyan, The origin of fluorescence from graphene oxide, Scientific reports, 2, 2012, 792.
5. V. Singh, D. Joung, L. Zhai, S. Das, S.I. Khondaker, S. Seal, Graphene based materials: past, present and future, Progress in materials science, 56, 8, 2011, 1178-1271.
6. Q. Xiang, J. Yu, M. Jaroniec, Graphene-based semiconductor photocatalysts, Chemical Society Reviews, 41, 2, 2012, 782-796.
7. X. Li, X. Wang, L. Zhang, S. Lee, H. Dai, Chemically derived, ultrasmooth graphene nanoribbon semiconductors, Science, 319, 5867, 2008, 1229-1232.
8. Y. Zhang, Y.-W. Tan, H.L. Stormer, P. Kim, Experimental observation of the quantum Hall effect and Berry's phase in graphene, Nature, 438, 7065, 2005, 201-204.
9. F. Bonaccorso, Z. Sun, T. Hasan, A. Ferrari, Graphene photonics and optoelectronics, Nature photonics, 4, 9, 2010, 611-622.
10. A. Kuzmenko, E. Van Heumen, F. Carbone, D. Van Der Marel, Universal optical conductance of graphite, Physical review letters, 100, 11, 2008, investigated 117401.
11. S. Schöche, N. Hong, M. Khorasaninejad, A. Ambrosio, E. Orabona, P. Maddalena, F. Capasso, Optical

properties of graphene oxide and reduced graphene oxide determined by spectroscopic ellipsometry, Applied Surface Science, 2017.

12. M. Goumri, B. Lucas, B. Ratier, M. Baitoul, Electrical and optical properties of reduced graphene oxide and multi-walled carbon nanotubes based nanocomposites: A comparative study, Optical Materials, 60, 2016, 105-113.

13. D.W. Boukhvalov, M.I. Katsnelson, Modeling of graphite oxide, Journal of the American Chemical Society, 130, 32, 2008, 10697-10701.

14. P. Johari, V.B. Shenoy, Modulating optical properties of graphene oxide: role of prominent functional groups, ACS nano, 5, 9, 2011, 7640-7647.

15. W. Fan, X. Yu, H.-C. Lu, H. Bai, C. Zhang, W. Shi, Fabrication of TiO 2 /RGO/Cu 2 O heterostructure for photoelectrochemical hydrogen production, Applied Catalysis B: Environmental, 181, 2016, 7-15.

16. Y. Hou, F. Zuo, A. Dagg, P. Feng, Visible Light-Driven α-Fe2O3 Nanorod/Graphene/BiV1–x Mo x O4 Core/Shell Heterojunction Array for Efficient Photoelectrochemical Water Splitting, Nano letters. 12, 12, 2012, 6464-6473.

17. N. Zhang, M.-Q. Yang, S. Liu, Y. Sun, Y.-J. Xu, Waltzing with the versatile platform of graphene to synthesize composite photocatalysts, Chemical reviews, 115, 18, 2015, 10307-10377.

18. P. Qiu, B. Park, J. Choi, M. Cui, J. Kim, J. Khim, BiVO4/Bi2O3 heterojunction deposited on graphene for an enhanced visible-light photocatalytic activity, Journal of Alloys and Compounds, 706, 2017, 7-15.

19. R. Beura, P. Thangadurai, Structural, optical and photocatalytic properties of graphene-ZnO nanocomposites for varied compositions, Journal of Physics and Chemistry of Solids, 102, 2017, 168-177.

20. W. Li, X.-Z. Tang, H.-B. Zhang, Z.-G. Jiang, Z.-Z. Yu, X.-S. Du, Y.-W. Mai, Simultaneous surface functionalization and reduction of graphene oxide with octadecylamine for electrically conductive polystyrene composites, Carbon, 49, 14, 2011, 4724-4730.

21. Z. Lin, Y. Liu, C.-p. Wong, Facile fabrication of superhydrophobic octadecylamine-functionalized graphite oxide film, Langmuir, 26, 20, 2010, 16110-16114.

22. H. Pang, Y.-Y. Piao, C.-H. Cui, Y. Bao, J. Lei, G.-P. Yuan, C.-L. Zhang, Preparation and performance of segregated polymer composites with hybrid fillers of octadecylamine functionalized graphene and carbon nanotubes, Journal of Polymer Research, 20, 11, 2013, 304.

23. B.R. Cruz-Ortiz, J.W. Hamilton, C. Pablos, L. Díaz-Jiménez, D.A. Cortés-Hernández, P.K. Sharma, M. Castro-Alférez, P. Fernández-Ibañez, P.S. Dunlop, J.A. Byrne, Mechanism of photocatalytic disinfection using titania-graphene composites under UV and visible irradiation, Chemical Engineering Journal, 316, 2017, 179-186.

24. H. Zhang, X. Lv, Y. Li, Y. Wang, J. Li, P25-graphene composite as a high performance photocatalyst, ACS nano, 4, 1, 2009, 380-386.

25. Y. Zhang, C. Pan, TiO2/graphene composite from thermal reaction of graphene oxide and its photocatalytic activity in visible light, Journal of Materials Science, 46, 8, 2011, 2622-2626.

26. S. Khan, J. Ali, M. Husain, M. Zulfequar, Synthesis of reduced graphene oxide and enhancement of its electrical and optical properties by attaching Ag nanoparticles, Physica E: Low-dimensional Systems and Nanostructures, 81, 2016, 320-325.

27. A. Jamshidi, M.O. Hamzah, Z. You, Performance of warm mix asphalt containing Sasobit®: State-of-the-art, Construction and Building Materials, 38, 2013, 530-553.

28. A. Syroezhko, M. Baranov, S. Ivanov, N. Maidanova, Influence of natural additives and those synthesized by the Fischer-Tropsch method on the properties of petroleum bitumen and quality of floated asphalt, Coke and Chemistry 54, 1, 2011, 26-31.

29. A. Sampath, Comprehensive evaluation of four warm asphalt mixture regarding viscosity, tensile strength, moisture sensitivity, dynamic modulus and flow number, The University of Iowa, 2010.

30. S. Mousavi, H. Esmaeili, O. Arjmand, S. Karimi, S. Hashemi, Biodegradation Study of Nanocomposites of Phenol Novolac Epoxy/Unsaturated Polyester Resin/Egg Shell Nanoparticles Using Natural Polymers, Journal of Materials, 2015, 2015.

31. S. Mousavi, A. Aghili, S. Hashemi, N. Goudarzian, Z. Bakhoda, S. Baseri, Improved Morphology and Properties of Nanocomposites, Linear Low Density Polyethylene, Ethylene-co-vinyl Acetate and Nano

Clay Particles by Electron Beam, Polymers from Renewable Resources, 7, 4, 2016, 135.

32. S. Mousavi, O. Arjmand, S. Hashemi, N. Banaei, Modification of the Epoxy Resin Mechanical and Thermal Properties with Silicon Acrylate and Montmorillonite Nanoparticles, Polymers from Renewable Resources, 7, 3, 2016, 101.

33. S.M. Mousavi, S.A. Hashemi, S. Jahandideh, S. Baseri, M. Zarei, S. Azadi, Modification of Phenol Novolac Epoxy Resin and Unsaturated Polyester Using Sasobit and Silica Nanoparticles, Polymers from Renewable Resources, 8, 3, 2017, 117.

34. S.A. Hashemi, S.M. Mousavi, R. Faghihi, M. Arjmand, S. Sina, A.M. Amani, Lead Oxide-Decorated Graphene Oxide/Epoxy Composite towards X-Ray Radiation Shielding, Radiation Physics and Chemistry, 2018.

35. S.A. Hashemi, S.M. Mousavi, Effect of bubble based degradation on the physical properties of Single Wall Carbon Nanotube/Epoxy Resin composite and new approach in bubbles reduction, Composites Part A: Applied Science and Manufacturing 90 (2016) 457-469.

36. S.A. Hashemi, S.M. Mousavi, R. Faghihi, M. Arjmand, S. Sina, A.M. Amani, Lead Oxide-Decorated Graphene Oxide/Epoxy Composite towards X-Ray Radiation Shielding, Radiation Physics and Chemistry.

37. A.M. Amani, S.A. Hashemi, S.M. Mousavi, H. Pouya, V. Arash, Electric Field Induced Alignment of Carbon Nanotubes: Methodology and Outcomes.

38. S.M. Mousavi, S.A. Hashemi, M. Arjmand, A.M. Amani, F. Sharif, S. Jahandideh, Octadecyl Amine Functionalized Graphene Oxide towards Hydrophobic Chemical Resistant Epoxy Nanocomposites, Chemistry Select, 3, 25, 2018, 7200-7207.

39. N. Goudarzian, S.A. Hashemi, M. Mirjalili, Un-saturated polyester resins modified with cresol novolac epoxy and silica nanoparticles: Processing and mechanical properties, International Journal of Chemical and Petroleum Sciences, 5, 1, 2016, 13-26.

40. S.M. Mousavi, S.A. Hashemi, A.M. Amani, H. Saed, S. Jahandideh, F. Mojoudi, Polyethylene Terephthalate/Acryl Butadiene Styrene Copolymer Incorporated with Oak Shell, Potassium Sorbate and Egg Shell Nanoparticles for Food Packaging Applications: Control of Bacteria Growth, Physical and Mechanical Properties, Polymers from Renewable Resources, 8, 4, 2017, 177-196.

41. D.C. Marcano, D.V. Kosynkin, J.M. Berlin, A. Sinitskii, Z. Sun, A. Slesarev, L.B. Alemany, W. Lu, J.M. Tour, Improved synthesis of graphene oxide, ACS nano, 4, 8, 2010, 4806-4814.

42. S.A. Hashemi, S.M. Mousavi, M. Arjmand, N. Yan, U. Sundararaj, Electrified single-walled carbon nanotube/epoxy nanocomposite via vacuum shock technique: Effect of alignment on electrical conductivity and electromagnetic interference shielding, Polymer Composites.

43. M.K. Shin, B. Lee, S.H. Kim, J.A. Lee, G.M. Spinks, S. Gambhir, G.G. Wallace, M.E. Kozlov, R.H. Baughman, S.J. Kim, Synergistic toughening of composite fibres by self-alignment of reduced graphene oxide and carbon nanotubes, Nature communications, 3, 2012, 650.

44. K. Tanaka, S. Iijima, Carbon Nanotubes and Graphene, 2010.

45. M.S. Dresselhaus, G. Dresselhaus, R. Saito, A. Jorio, Raman spectroscopy of carbon nanotubes, Physics reports, 409, 2, 2005, 47-99.

46. R. Saito, M. Hofmann, G. Dresselhaus, A. Jorio, M. Dresselhaus, Raman spectroscopy of graphene and carbon nanotubes, Advances in Physics, 60, 3, 2011, 413-550.